

Evaluation of accurate uncertainty of measurement in L subshell ionization cross-section

Shashank Singh^a, Soumya Chatterjee^b, D. Mitra^b, T. Nandi^c

^a*Department of Physics, Panjab University, Chandigarh-160014, India.*

^b*Department of Physics, University of Kalyani, Kalyani, West Bengal-741235, India.*

^c*1003 Regal, Mapsko Royal Ville, Sector 82, Gurugram-122004, Haryana, India.*

correspondence: nanditapan@gmail.com

Superannuated from Inter-University Accelerator Centre, Aruna Asaf Ali Marg, New Delhi-110067, India.

Abstract

To have a better understanding of a physical process, a comparison of experimental data with theoretical values is mandatory. The comparison is meaningful if the uncertainty in the experiment is accounted well. However, it is seldom seen, especially for a complex phenomenon. We take a test case through L subshell ionization of atoms by particle impact. **Experimentally, x-ray production cross-sections are measured, but ionization cross-sections are calculated theoretically.** Furthermore, the uncertainty of the x-ray production cross-section is mainly statistics and detector-efficiency driven. But ionization cross-section involves many other factors because of the relationship between the production and ionization cross section, having wide uncertainty spectrum. Consequently, determining the measurement uncertainty in L subshell ionization cross-section is always difficult. We have studied this issue in the simplest way, where the rule of weighted propagation of relative uncertainty is utilised. We notice that larger uncertainties are involved in atomic parameters relevant to L_1 ($2s_{1/2}$) subshell than those associated with the other two L_2 ($2p_{1/2}$) and L_3 ($2p_{3/2}$) subshells. **Hence, comparison between theory and experiment would give higher emphasis on L_2 and L_3 subshell ionization cross sections.** We believe this work aware us that the appropriate uncertainty evaluation is extremely important for providing the right judgment on the data.

Keywords: , Accurate uncertainty evaluation, L subshell Ionization cross-section, weighted propagation of uncertainty, best experimental

technique suggested, achieving full confidence on the results

1. Introduction

According to the “International Vocabulary of Basic and General Terms in Metrology” a measurement is defined as a “set of operations having the object of determining a value of a quantity” [1]. Therefore, a result of a measurement is an estimate of the value of a measurand and should be accompanied by an uncertainty statement [2]. The uncertainty of measurement is the doubt that exists about the result of any measurement. But for every measurement - even the most careful - there is always a margin of doubt. It is a complicated subject, and still evolving. So there is a great need for a guide that provides clear, down-to-earth explanations, easy enough for non-expert readers [3]. **While error is the difference between the measured value and the ‘true value’ of the quantity being measured.** The ‘true’ value can only be found from a very large set of measurements and thus any uncertainty whose value is not known is a measure of uncertainty. Hence, only an estimate of the standard deviation can be found from a moderate number of values and one standard deviation is an estimate of the uncertainty. The “Guide to the Expression of Uncertainty of Measurement” (GUM) provides the general rules for quantifying the uncertainty in a measurement [4]. As a rule of thumb usually between 4 and 10 readings is sufficient to make a good quality measurement and its uncertainty.

The uncertainty evaluation is an important part of a good quality measurement. It is only complete if it is accompanied by a statement of the uncertainty. A measurand Y is determined from N other quantities X_i using a functional relationship as follows

$$Y = f(X_1, X_2, \dots, X_N) \quad (1)$$

where the quantities X_1, X_2, \dots, X_N may themselves be viewed as measurands and may depend on other quantities like $X_i = f(x_i)$. Two approaches based on the evaluation method are used to estimate the standard uncertainty: Type A evaluation is based on statistical treatment on a series of observations, and Type B evaluation is based on non-statistical one such as data from manufacturer’s specifications, previous experimental data, theoretical data, etc. Note that both Type A and Type B uncertainties can be due to a “random effect” as well as to a “systematic effect” in nature. Random effect is recognizable from the variations in the repeated observations,

where uncertainty analysis of the observed data is governed by the rules of statistics. On the other hand, though the contribution of systematic effect appears in the repeated measurements, but we can learn nothing from these. Other methods are needed to estimate the uncertainties due to systematic effects.

Inner shell ionization of an atom is a very interesting field of study for the theoreticians as well as experimentalists since last century. For a better understanding of the inner shell ionization process, a lot of work had been reported using different experimental pathways. In this endeavour, inner shell ionization induced by electron [5, 6, 7, 8, 9, 10, 11, 12], photon [13, 14, 15, 16, 17, 18], proton [19, 20, 21, 22, 23, 24, 25, 26, 27] and varieties of heavy ions [28, 29, 30, 31, 30, 32, 33, 34, 35, 36, 37, 38, 39, 40] had been reported. To explain the ionization processes, various theories like SCA [41], PWBA [42], ECPSSR [43, 44, 45, 46, 47], ECUSAR [45] and SLPA [48] have been used. In a lot of studies, comparisons were made between the experimental cross-section data and corresponding theoretical predictions. Accuracy of experimental data is very important. Given uncertainty alongside the data gives the accuracy of such measurement. Finite uncertainty in the x-ray production cross-section data is indispensable due to the uncertainty in photo-peak area evaluation, efficiency of the detector, ion beam current, target thickness, etc. The ionization cross-sections can be extracted from the measured x-ray production cross-sections using suitable atomic parameters. Uncertainties in the x-ray production cross-sections and the used atomic parameters are propagated into the ionization cross-sections. Conversion of K shell x-ray production cross-section into the ionization cross-section requires only one atomic parameter, fluorescence yield [49], hence evaluating the uncertainty is simple. In contrast, obtaining the L subshell ionization cross-section from the x-ray production cross-section data requires several atomic parameters including fluorescence yield, Coster-Kronig yield, the fraction of radiative transition rates, which in turn introduce the Type B uncertainty. Thus, the calculation of uncertainty is complex and significant discrepancies prevalent in literature. To examine the reason behind such large variation, we have made a thorough study of the propagation of uncertainties from the L x-ray production cross-sections to the L subshell ionization cross-section. Details will be seen in the next section, where the method of weighted uncertainty propagation rule has been applied. For example, we have taken results from recent work Oswal *et al.* [40] and assessed the quoted accuracy. More so, an attempt is put on suggesting the best possible way to perform

the most accurate experiment. Probably, besides the L subshell ionization, this work will be a general guideline for uncertainty analysis of many other measurements relevant to physics or beyond.

2. Present scenario of measurement uncertainty in L-shell ionization studies

In the past, many experiments have studied the L-shell ionization in various targets bombarded by different projectiles in certain energy ranges and quoted the measurement uncertainties. A brief list is given in the table 2. Though the experiments have followed similar detection systems, but the measurement uncertainties vary in a wide range of 4-35%. This scenario is a deterrent for improving the theoretical understanding.

Table 1: Uncertainties quoted for L shell production and ionization cross sections in earlier experiments.

Ref.	Targets	Projectile, its energy	$\delta L_1, \delta L_2, \delta L_3$ (%)	Remarks
Chang [50]	W	electron, 11-40 keV	17, 15, 15	Nearly equal uncertainties for all subshells
Palinkas and Schlenk [51]	Au, Pb, Bi	electron, 60-600 keV	22, 15, 11	7-10% uncertainties for x-ray production cross sections for all the three elements
Reusch <i>et al.</i> [52]	$29 \leq Z \leq 79$	electron, 50-200 keV	7-15, 6-15, 6-15	Nearly same uncertainties for all the subshells and about 15% for total L ionization cross section
Carvalho <i>et al.</i> [53]	W	electron, 12-40 keV	–	10% uncertainty for σ_3/σ_2 and σ_2/σ_1
Llovet <i>et al.</i> [54]	$1 \leq Z \leq 99$	electrons and positron, up to 1 GeV	10-30, 10-30, 10-30	Similar uncertainties for all elements and all subshells
Barros <i>et al.</i> [55]	Au	electron, 50-100 keV	22, 11, 12	Without inclusion of uncertainties in atomic relaxation parameters
Barros <i>et al.</i> [55]	Au	electron, 50-100 keV	23, 12, 13	With inclusion of uncertainty in atomic relaxation parameters [56, 57, 58, 59]
Barros <i>et al.</i> [55]	Au	electron, 50-100 keV	28, 16, 16	With inclusion of uncertainty in atomic relaxation parameters as given in [60, 61, 56]
Bernstein and Lewis [62]	Ta, Au, Pb, U	H, 1.5-4.25 MeV	–	20% Uncertainty for all x-ray production cross-sections
Chang <i>et al.</i> [63]	Ta, Au, Bi	H, 1 to 5.5 and He, 1 to 11 MeV	22, 28, 21	Uncertainties for L_α is about 15%, for L_{γ_1+5} and L_{γ_2+3+4} are about 15-18%
Leite <i>et al.</i> [64]	Au, Tl, Pb, Bi, Th, U	H, 0.5-3.5 MeV	–	7% uncertainty for production cross section and error bar for ionization cross sections given in figures only
Wheeler <i>et al.</i> [65]	Pr, Sm, Tb, Ho, Yb	H, 150-400 keV	20, 20, 15	Same uncertainty for all the elements
Sokhi and Crumpton [66]	Different targets	H	6-20, 7-20, 6-26	Uncertainty differs with target
Miranda and Lapicki [67]	Ne to Am	H, 0 keV to 1 GeV	–	No regular trend seen in uncertainties
Semaniak <i>et al.</i> [68]	Between La to Au	^{14}N , 1.75-22.4 MeV	25-10, 25-15, 25-10	Uncertainties at low energy were 10-25% and 10% at high energies
Semaniak <i>et al.</i> [69]	$72 \leq Z \leq 90$	C and N, 0.4 to 1.8 MeV/amu	6-20, 5-12, 4-10	Uncertainties differs with target
Dhal <i>et al.</i> [70]	Au, Bi	B, 4.8-8.8 MeV	10, 10, 10	Same for both the elements
Banas <i>et al.</i> [71]	Au	O of 0.4-2.2 MeV/amu	15-30, 15-30, 15-30	10-20% for all production cross-section
Pajek <i>et al.</i> [72]	Au, Bi, Th, U	O, 6.4 to 70 MeV	–	Uncertainties for production cross-sections of $L_{\alpha 1,2}$ were 9%, for L_{γ_1} 13% and for $L_{\gamma_2,3}$ 10-25% and for subshell ionization cross section the error bars included in figure only
Fijał-Kirjczyk <i>et al.</i> [73]	Au and Bi	S, 12.8-120 MeV	10-30, 10-30, 10-30	Uncertainties for production cross-sections of $L_{\alpha 1,2}$ were 7-15%, for L_{γ_1} 10-18% and for $L_{\gamma_2,3}$ 15-25% for all elements
Oswal <i>et al.</i> [40]	Ta, Pt, Th, U	Si of 84-140 MeV	15-20 for Ta and 30-35 for other targets, 12-15, 12-15	10-12% for the production cross sections, uncertainties were evaluated quite satisfactorily

3. Measurement uncertainty evaluation method and results

A representative spectrum of emitted L x-rays induced by heavy particles is shown in Fig. 1. Thus, we determine the experimentally x-ray production cross-section for a particular x-ray peak (σ_x^i) using a relation

$$\sigma_x^i = \frac{Y_x^i A \text{Sin}\theta}{N_A \epsilon n_p t \beta} \quad (2)$$

where Y_x^i is the intensity of the i th x-ray peak, A is the atomic weight of the target, θ is the angle between the incident ion beam and the target foil normal, N_A is the Avogadro number, n_p is the number of incident projectiles, ϵ is the effective efficiency of the x-ray detector, t is the target thickness in $\mu\text{g}/\text{cm}^2$ and β is a correction factor for the absorption of the emitted x-rays inside the target. Measurement uncertainty on the σ_x^i is introduced due to uncertainties in different parameters used in Eqs. (2). Let us consider an experiment [40] to have ideas on the uncertainties involved, which are as follows: the photo peak area, Y_x^i , evaluation ($\leq 1\%$ for the L_α x-ray peak and $\approx 3\%$ for the other peaks), the ion beam current ($\approx 5\%$), $\text{Sin}\theta$ ($\approx 1\%$) and the target thickness ($\approx 3\%$). The uncertainty in the detector efficiency values, ϵ , is $\approx 8\%$ in the energy region of current interest. The relative combined standard uncertainty equation for the x-ray production cross-section as given in Eqs. (2) can be written including the relative combined variance and covariance as follows

$$\begin{aligned} \left(\frac{\delta\sigma_x^i}{\sigma_x^i}\right)^2 &= \left(\frac{\delta Y_x^i}{Y_x^i}\right)^2 + \left(\frac{\delta\epsilon}{\epsilon}\right)^2 + \left(\frac{\delta n_p}{n_p}\right)^2 + \left(\frac{\delta t}{t}\right)^2 + \left(\frac{\delta \text{Sin}\theta}{\text{Sin}\theta}\right)^2 + \left(\frac{\delta\beta}{\beta}\right)^2 \\ &+ 2 \delta t \delta\beta \frac{\delta\sigma_x^i}{\delta t} \frac{\delta\sigma_x^i}{\delta\beta} \frac{1}{\sigma_x^{i2}} - 2 \delta\epsilon \delta Y_x^i \frac{\delta\sigma_x^i}{\delta\epsilon} \frac{\delta\sigma_x^i}{\delta Y_x^i} \frac{1}{\sigma_x^{i2}} \end{aligned} \quad (3)$$

Last two terms in uncertainty arise due to the contributions coming from the covariance relationship of the detector efficiency (ϵ) with the i^{th} intensity peak (Y_x^i) and the absorption correction factor of the emitted x-rays inside the target (β) with the target thickness (t). Simplifying these two terms by the equation (2) we can write the equation (3) as under

$$\begin{aligned} \left(\frac{\delta\sigma_x^i}{\sigma_x^i}\right)^2 &= \left(\frac{\delta Y_x^i}{Y_x^i}\right)^2 + \left(\frac{\delta\epsilon}{\epsilon}\right)^2 + \left(\frac{\delta n_p}{n_p}\right)^2 + \left(\frac{\delta t}{t}\right)^2 + \left(\frac{\delta \text{Sin}\theta}{\text{Sin}\theta}\right)^2 + \left(\frac{\delta\beta}{\beta}\right)^2 \\ &+ 2 \frac{\delta\epsilon}{\epsilon} \frac{\delta Y_x^i}{Y_x^i} + 2 \frac{\delta t}{t} \frac{\delta\beta}{\beta} \end{aligned} \quad (4)$$

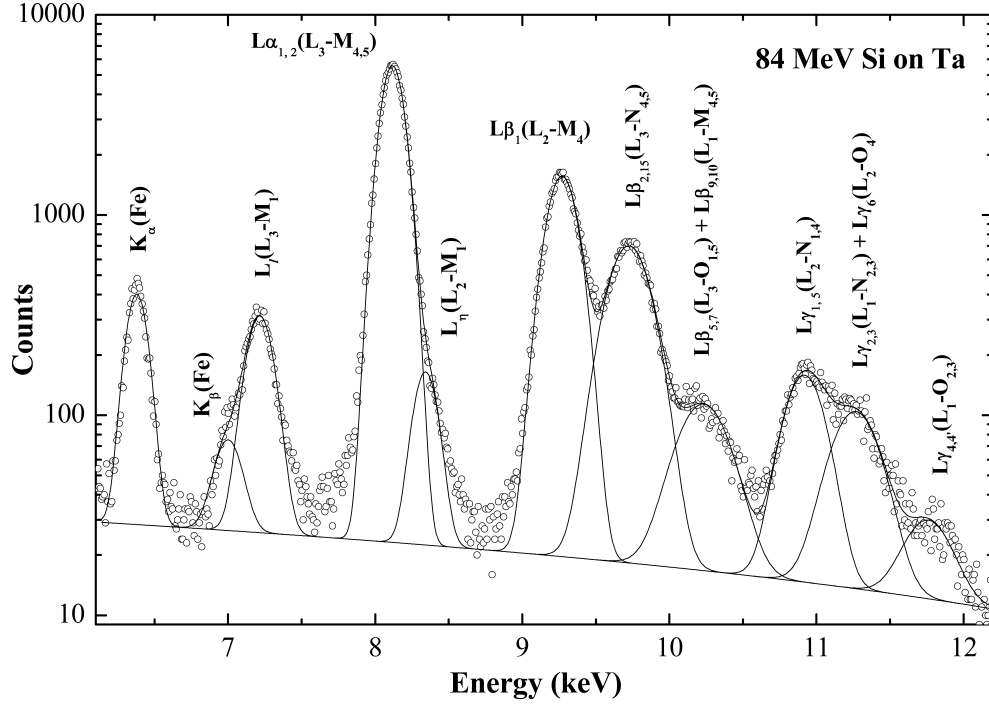


Figure 1: L x-ray spectra of ${}_{73}\text{Ta}$ bombarded with the 84 MeV ${}^{28}\text{Si}$ ions. Deconvoluted x-ray lines due to different transitions are shown along with the background due to Compton scattering.

Table 2: X-ray production cross-sections with uncertainty for the elements of our interest (uncertainties are obtained using the uncertainties on various parameters mentioned in [40] and given in terms of percentage).

El.	$\sigma_{L\gamma_{2+3}}$	$\sigma_{L\gamma_{1+5}}$	$\sigma_{L\alpha_{1+2}}$
${}_{73}\text{Ta}$	193 ± 12	290 ± 12	6614 ± 11
${}_{78}\text{Pt}$	154 ± 12	231 ± 12	5542 ± 11
${}_{90}\text{Th}$	42 ± 12	63 ± 12	1537 ± 11
${}_{92}\text{U}$	28 ± 12	42 ± 12	1098 ± 11

The absorption correction factor β is written as

$$\beta = \frac{1 - \exp^{-\mu t}}{\mu t} \quad (5)$$

and

$$\frac{\delta\beta}{\beta} \approx -\mu t \left(\frac{\delta t}{t} + \frac{\delta\mu}{\mu} \right). \quad (6)$$

Where, μ is for attenuation co-efficient inside the target. The unit of μ is cm^2/g and that of t is $\mu g/cm^2$; the value μt is very small. For instance, μ of carbon for Fe K_α energy (6.4 keV) is $8.73 cm^2/g$, $\frac{\delta\mu}{\mu} = 0.5\%$ [74] and if the target thickness is taken as $50 \mu g/cm^2$ and $\frac{\delta t}{t} = 3\%$, we get $\frac{\delta\beta}{\beta} = 0.0013\%$. Thus, $\frac{\delta\beta}{\beta}$ is negligibly small and the terms containing $\delta\beta$ can be equated to zero. With this circumstances, the equation (4) can be written as

$$\left(\frac{\delta\sigma_x^i}{\sigma_x^i} \right)^2 = \left(\frac{\delta Y_x^i}{Y_x^i} \right)^2 + \left(\frac{\delta\epsilon}{\epsilon} \right)^2 + \left(\frac{\delta n_p}{n_p} \right)^2 + \left(\frac{\delta t}{t} \right)^2 + \left(\frac{\delta \text{Sin}\theta}{\text{Sin}\theta} \right)^2 + 2 \frac{\delta\epsilon}{\epsilon} \frac{\delta Y_x^i}{Y_x^i} \quad (7)$$

Here we show that the ϵ does not have any relation with any quantities present in equation (2). The detector efficiency (ϵ) is written according to a semi empirical model [75] as

$$\epsilon = \frac{\Omega}{4\pi} \exp\left(-\sum_1^n \mu_i d_i\right) f_E (1 - \exp(-\mu_C D)) \quad (8)$$

where Ω is the fractional solid angle subtended by the detector crystal at the source and i denotes the medium between the source and the beryllium window, the window itself, a possible ice layer, the gold electrode, the frontal crystal dead layer etc. The d_i are the thickness of these absorbers and μ_i are their linear absorption coefficients taken from XCOM database [76]. The term f_E represents the escape peak correction factor. The μ_C is the photoelectric absorption coefficient of the detector crystal of thickness D . There is no quantity present in RHS of equation (2) is present in the above equation. Hence, ϵ does not have obvious covariance with another quantity. However, the magnitude of Y_x^i is strongly affected by the value of ϵ and $\epsilon = f(E)$, E =energy of x-ray, hence, the ϵ is having relation with Y_x^i . Whereas Y_x^i is

directly proportional to the number of projectiles (N_p) as well as the target thickness (t). Hence, ϵ does not have covariance with the Y_i^x and no covariance with either N_p and t .

The measured L x-ray production cross-sections are given in Table 2. To calculate the ionization cross-section from the x-ray production cross-section, we need appropriate relation between these two. It is a simple relation for the K shell case involving only fluorescence yield: $\sigma_K = \sigma_x \omega_K$, where σ_K is the K shell ionization cross-section, σ_x is the K x-ray production cross-section, ω_K is the K x-ray fluorescence yield [77]. However, the ionization cross-sections of different L subshells [32, 78] are related to the x-ray production cross-sections through the following relations involving several atomic parameters like the fraction of radiative transition rates, fluorescence yields corresponding to L_i subshells (ω_i) and Coster-Kronig transition probability (f_{ij}) between two subshells i and j is written as follows

$$\sigma_{L_1} = \frac{\sigma_{L\gamma_{2+3}}}{\omega_1 S_{\gamma_{2+3,1}}}. \quad (9)$$

where σ_{L_1} is the L_1 subshell ionization cross-section, $S_{\gamma_{2+3,1}}$ is the fraction of radiative transition rates for $L_{\gamma_{2+3}}$ and ω_1 is fluorescence yield of all the transitions terminating at L_1 . Similarly, the L_2 subshell ionization cross-section σ_{L_2} is given as

$$\sigma_{L_2} = \frac{\sigma_{L\gamma_{1+5}}}{\omega_2 S_{\gamma_{1+5,2}}} - \sigma_{L_1} f_{12}. \quad (10)$$

Where $S_{\gamma_{1+5,1}}$ is the fraction of radiative transition rates for $L_{\gamma_{1+5}}$, ω_2 is fluorescence yield of all the transitions terminating at L_2 and f_{12} is the Coster-Kronig transition because of vacancy transfer from L_1 to L_2 . Lastly, the L_3 subshell ionization cross-section σ_{L_3} is given as

$$\sigma_{L_3} = \frac{\sigma_{L\alpha_{1+2}}}{\omega_3 S_{\alpha_{1+2,3}}} - \sigma_{L_1} (f_{12} f_{23} + f_{13}) - \sigma_{L_2} f_{23}. \quad (11)$$

Where $S_{\alpha_{1+2,1}}$ is the fraction of radiative transition rates, $L_{\alpha_{1+2}}$, ω_3 is fluorescence yield of all the transitions terminating at L_3 , f_{13} is the Coster-Kronig transition because of vacancy transfer from L_1 to L_3 , and f_{23} is the Coster-Kronig transition because of vacancy transfer from L_2 to L_3 .

We can notice that obtaining σ_{L_1} from Eqs. (9) is simpler than finding $\sigma_{L_{2,3}}$ from Eqs. (10) and Eqs. (11), respectively, as Eqs. (8) does not contain any Coster-Kronig transition probability. Whereas Eqs. (10) and Eqs. (11) contain one f_{ij} and three f_{ij} s, respectively. The value of ω 's and f 's are taken from Campbell et al. [79, 80] and the value of emission rates are taken from Campbell and Wang [59] for obtaining the fraction of radiative transition rates. The emission rates of L_1 , L_2 and L_3 subshells for the elements of our interest are given below in Table 3, where, L_1M_3 etc., denote the origin of x-ray transition. For example, L_1M_3 is due to an electron jumping from M_3 to vacant L_1 subshell. L_3O_{45} denotes a pair of emissions from O_{45} to vacant L_1 subshell having line energies very close. For all the emission rate data, the uncertainty reported [59] is 0.2%. Using these emission rates, we can calculate the fraction of radiative transition rates when two or more lines are measured as a single line due to limited resolving power of detector used. Since $L_{\gamma_{2+3}}$ line is due to L_{γ_2} (L_1N_2) and L_{γ_3} (L_1N_3) transitions, so the fraction of radiative transition rates for $L_{\gamma_{2+3}}$ line is written as

$$S_{\gamma_{2+3,1}} = \frac{L_1N_2 + L_1N_3}{\sum_i L_1X_i} = \frac{L_1N_2}{\sum_i L_1X_i} + \frac{L_1N_3}{\sum_i L_1X_i} \quad (12)$$

Now, uncertainty equation for the $S_{\gamma_{2+3,1}}$ can be written as

$$\left(\frac{\delta S_{\gamma_{2+3,1}}}{S_{\gamma_{2+3,1}}}\right)^2 = \left(\frac{\delta L_1N_2}{L_1N_2}\right)^2 + \left(\frac{\delta L_1N_3}{L_1N_3}\right)^2 + 2\left(\frac{\sum_i \delta L_1X_i}{\sum_i L_1X_i}\right)^2 \quad (13)$$

Similarly, we can calculate $S_{\gamma_{1+5,2}}$ and $S_{\alpha_{1+2,3}}$. Since $L_{\gamma_{1+5}}$ line is due to L_{γ_1} (L_2N_4) and L_{γ_5} (L_2N_1) transitions so the fraction of radiative transition rates for for $L_{\gamma_{1+5}}$ line is

$$S_{\gamma_{1+5,1}} = \frac{L_2N_4 + L_2N_1}{\sum_i L_2Y_i} = \frac{L_2N_4}{\sum_i L_2Y_i} + \frac{L_2N_1}{\sum_i L_2Y_i}. \quad (14)$$

$L_{\alpha_{1+2}}$ line is due to L_{α_1} (L_3M_4) and L_{α_2} (L_3M_5) transitions so the fraction of radiative transition rates for $L_{\alpha_{1+2}}$ line is:

$$S_{\alpha_{1+2,3}} = \frac{L_3M_4 + L_3M_5}{\sum_i L_3Z_i} = \frac{L_3M_4}{\sum_i L_3Z_i} + \frac{L_3M_5}{\sum_i L_3Z_i}. \quad (15)$$

Table 3: L_1 , L_2 and L_3 emission rates for electric dipole transitions [59] are listed with multiplication factor 10^{-2} . All rates are primarily in eV/h ($= 1.519 \times 10^{15} S^{-1}$), hence rates in the table are in unit of $1.519 \times 10^{13} S^{-1}$.

El.	L_1L_3	L_1M_2	L_1M_3	L_1N_2	L_1N_3	L_1O_{23}	L_1P_{23}		
${}_{73}Ta$	1.446	24.65	31.54	6.176	8.386	2.189			
${}_{78}Pt$	2.636	34.94	41.27	9.023	11.54	3.561			
${}_{90}Th$	10.82	75.68	69.68	20.75	21.87	10.10	2.004		
${}_{92}U$	13.62	85.59	74.82	23.63	23.93	11.56	2.146		
El.	L_2M_1	L_2M_4	L_2N_1	L_2N_4	L_2O_1	L_2O_4	L_2P_1		
${}_{73}Ta$	2.928	107.4	0.7266	21.02	0.1256	0.4713	0.01584		
${}_{78}Pt$	4.061	148.0	1.038	30.63	0.2039	2.772	0.01050		
${}_{90}Th$	8.374	295.1	2.283	68.56	0.5646	13.35	0.1240		
${}_{92}U$	9.375	328.0	2.580	77.63	0.6538	15.59	0.1397		
El.	L_3M_1	L_3M_4	L_3M_5	L_3N_1	L_3N_4	L_3N_5	L_3O_1	L_3O_{45}	L_3P_1
${}_{73}Ta$	4.378	9.655	85.06	1.054	1.772	15.88	0.1809	0.3825	0.0227
${}_{78}Pt$	6.377	13.11	115.3	1.569	2.511	22.61	0.3051	2.176	0.01513
${}_{90}Th$	14.67	25.02	219.5	3.773	5.192	47.40	0.9264	9.983	0.2009
${}_{92}U$	16.72	27.58	241.8	4.314	5.796	53.13	1.076	11.50	0.2299

All calculated fraction of radiative transition rates for elements of our interest are given in Table 4. Uncertainty equation for $S_{\gamma_{1+5,1}}$ and $S_{\alpha_{1+2,3}}$ can also be written in terms of Eqs. (11). Emission rates and corresponding uncertainties are known [59], so we can calculate uncertainty in every fraction of radiative transition rates as shown in Table 4 for the elements of our interest.

Now, from Eqs. (8), the uncertainty equation for σ_{L_1} can be written as:

Table 4: The fraction of radiative transition rates for the elements of our interest (uncertainties are given in percentage).

El.	$S_{\gamma_{2+3,1}}$	$S_{\gamma_{1+5,2}}$	$S_{\alpha_{1+2,3}}$
${}_{73}Ta$	0.1957 ± 1	0.1639 ± 1	0.8000 ± 1
${}_{78}Pt$	0.1997 ± 1	0.1696 ± 1	0.7831 ± 1
${}_{90}Th$	0.2020 ± 1	0.1824 ± 1	0.7485 ± 1
${}_{92}U$	0.2021 ± 1	0.1848 ± 1	0.7437 ± 1

Table 5: σ_{L_1} (barns/atom) along with uncertainties for various target atoms by Si beams at 84 MeV. Corresponding values of $\sigma_{L_{\gamma_{2+3}}}$ (barns/atom) [40], conversion parameters ω_1 [79, 80] and $S_{\gamma_{2+3,1}}$ are also given (uncertainties given in percentage).

El.	$\sigma_{L_{\gamma_{2+3}}}$	ω_1	$S_{\gamma_{2+3,1}}$	σ_{L_1}
${}_{73}\text{Ta}$	193 ± 12	0.144 ± 15	0.1957 ± 1	6858 ± 19
${}_{78}\text{Pt}$	154 ± 12	0.114 ± 30	0.1997 ± 1	6756 ± 32
${}_{90}\text{Th}$	42 ± 12	0.159 ± 35	0.2020 ± 1	1308 ± 37
${}_{92}\text{U}$	28 ± 12	0.168 ± 35	0.2021 ± 1	819 ± 37

$$\left(\frac{\delta\sigma_{L_1}}{\sigma_{L_1}}\right)^2 = \left(\frac{\delta\sigma_{L_{\gamma_{2+3}}}}{\sigma_{L_{\gamma_{2+3}}}}\right)^2 + \left(\frac{\delta\omega_1}{\omega_1}\right)^2 + \left(\frac{S_{\gamma_{2+3,1}}}{S_{\gamma_{2+3,1}}}\right)^2 \quad (16)$$

Value of $\sigma_{L_{\gamma_{2+3}}}$ (barns/atom), ω_1 and $S_{\gamma_{2+3,1}}$ with uncertainties, required for calculation of uncertainty of σ_{L_1} , are given in Table 5. Uncertainty of $\sigma_{L_{\gamma_{2+3,1}}}$ is taken from Table 2, that of ω_1 is taken from [79, 80] and that of $S_{\gamma_{2+3,1}}$ is taken from Table 4. Values of the σ_{L_1} along with the uncertainties are given in Table 5.

Now, Eqs. (10) can be written as

$$\sigma_{L_2} = \sigma_{L_2}^A + \sigma_{L_2}^B$$

where,

$$\sigma_{L_2}^A = \frac{\sigma_{L_{\gamma_{1+5}}}}{\omega_2 S_{\gamma_{1+5,2}}}, \sigma_{L_2}^B = -\sigma_{L_1} f_{12}$$

So, the uncertainty equation for σ_{L_2} can be written as

$$\left(\frac{\delta\sigma_{L_2}}{\sigma_{L_2}}\right)^2 = \left(\frac{\sigma_{L_2}^A}{\sigma_{L_2}}\right)^2 \left(\frac{\delta\sigma_{L_2}^A}{\sigma_{L_2}^A}\right)^2 + \left(\frac{\sigma_{L_2}^B}{\sigma_{L_2}}\right)^2 \left(\frac{\delta\sigma_{L_2}^B}{\sigma_{L_2}^B}\right)^2 \quad (17)$$

where,

$$\left(\frac{\delta\sigma_{L_2}^A}{\sigma_{L_2}^A}\right)^2 = \left(\frac{\delta\sigma_{L_{\gamma_{1+5}}}}{\sigma_{L_{\gamma_{1+5}}}}\right)^2 + \left(\frac{\delta\omega_2}{\omega_2}\right)^2 + \left(\frac{\delta S_{\gamma_{1+5,2}}}{S_{\gamma_{1+5,2}}}\right)^2 \quad (17.1)$$

Table 6: σ_{L_2} (barns/atom) along with uncertainties for various target atoms by Si beams of 84 MeV. Corresponding values of $\sigma_{L_{\gamma_{1+5}}}$ (barns/atom) [40], conversion parameters ω_2 , f_{12} [79, 80] and $S_{\gamma_{1+5,2}}$ [59] are also given (uncertainties given in percentage).

Elements	$\sigma_{L_{\gamma_{1+5}}}$	ω_2	$S_{\gamma_{1+5,2}}$	f_{12}	σ_{L_2}
${}_{73}Ta$	290 ± 12	0.28 ± 5	0.1639 ± 1	0.118 ± 20	5510 ± 16
${}_{78}Pt$	231 ± 12	0.344 ± 5	0.1696 ± 1	$0.075 \pm 30-40$	3448 ± 17
${}_{90}Th$	63 ± 12	0.503 ± 5	0.1824 ± 1	$0.040 \pm 50-100$	635 ± 15
${}_{92}U$	42 ± 12	0.506 ± 5	0.1848 ± 1	$0.035 \pm 50-100$	417 ± 15

and

$$\left(\frac{\delta\sigma_{L_2}^B}{\sigma_{L_2}^B}\right)^2 = \left(\frac{\delta\sigma_{L_1}}{\sigma_{L_1}}\right)^2 + \left(\frac{\delta f_{12}}{f_{12}}\right)^2 \quad (17.2)$$

Values of $\sigma_{L_{\gamma_{1+5}}}$ (barns/atom), ω_2 , $S_{\gamma_{1+5,2}}$ and f_{12} with uncertainties, required for calculation of uncertainty for σ_{L_2} are given in Table 6. σ_{L_1} along with its uncertainty is taken from Table 5. 10% uncertainty in production cross-section ($\sigma_{L_{\gamma_{1+5,2}}}$) is taken, which is due to the uncertainty in the photopeak area evaluation ($\approx 4\%$), the ion beam current ($\approx 5\%$) and the target thickness ($\approx 3\%$) [40]. The uncertainty in the effective efficiency values is 5-8% in the energy region of current interest [40], highest value 8% is taken. Uncertainty for ω_2 is 5% for all element of our interest [79, 80]. For f_{12} , uncertainty for ${}_{73}Ta$ is 20%, for ${}_{78}Pt$ is 30-40%, for ${}_{90}Th$ is 50-100% and for ${}_{92}U$ is 50-100% [79, 80]. $\delta S_{\gamma_{1+5,2}}$ is due to uncertainty in the emission rate, which is only 0.2% [59]. Values of σ_{L_2} with uncertainties is given in Table 6.

Similarly, the Eqs. (11) can be written as

$$\sigma_{L_3} = \sigma_{L_3}^C + \sigma_{L_3}^D + \sigma_{L_3}^E + \sigma_{L_3}^F$$

So the uncertainty equation can be written as

$$\left(\frac{\delta\sigma_{L_3}}{\sigma_{L_3}}\right)^2 = \left(\frac{\sigma_{L_3}^C}{\sigma_{L_3}}\right)^2 \left(\frac{\delta\sigma_{L_3}^C}{\sigma_{L_3}^C}\right)^2 + \left(\frac{\sigma_{L_3}^D}{\sigma_{L_3}}\right)^2 \left(\frac{\delta\sigma_{L_3}^D}{\sigma_{L_3}^D}\right)^2 + \left(\frac{\sigma_{L_3}^E}{\sigma_{L_3}}\right)^2 \left(\frac{\delta\sigma_{L_3}^E}{\sigma_{L_3}^E}\right)^2 + \left(\frac{\sigma_{L_3}^F}{\sigma_{L_3}}\right)^2 \left(\frac{\delta\sigma_{L_3}^F}{\sigma_{L_3}^F}\right)^2 \quad (18)$$

where,

$$\sigma_{L_3}^C = \frac{\sigma_{L_{\alpha_1+2}}}{\omega_3 S_{\alpha_1+2,3}}, \sigma_{L_3}^D = -\sigma_{L_1}(f_{12}f_{23}), \sigma_{L_3}^E = -\sigma_{L_1}f_{13}, \sigma_{L_3}^F = -\sigma_{L_2}f_{23}$$

and the corresponding uncertainty equations as follows

$$\left(\frac{\delta\sigma_{L_3}^C}{\sigma_{L_3}^C}\right)^2 = \left(\frac{\delta\sigma_{L_{\alpha_1+2}}}{\sigma_{L_{\alpha_1+2}}}\right)^2 + \left(\frac{\delta\omega_3}{\omega_3}\right)^2 + \left(\frac{\delta S_{\alpha_1+2,3}}{S_{\alpha_1+2,3}}\right)^2 \quad (18.1)$$

$$\left(\frac{\delta\sigma_{L_3}^D}{\sigma_{L_3}^D}\right)^2 = \left(\frac{\delta\sigma_{L_1}}{\sigma_{L_1}}\right)^2 + \left(\frac{\delta f_{12}}{f_{12}}\right)^2 + \left(\frac{\delta f_{23}}{f_{23}}\right)^2 \quad (18.2)$$

$$\left(\frac{\delta\sigma_{L_3}^E}{\sigma_{L_3}^E}\right)^2 = \left(\frac{\delta\sigma_{L_1}}{\sigma_{L_1}}\right)^2 + \left(\frac{\delta f_{13}}{f_{13}}\right)^2 \quad (18.3)$$

and

$$\left(\frac{\delta\sigma_{L_3}^F}{\sigma_{L_3}^F}\right)^2 = \left(\frac{\delta\sigma_{L_2}}{\sigma_{L_2}}\right)^2 + \left(\frac{\delta f_{23}}{f_{23}}\right)^2 \quad (18.4)$$

Values of $\sigma_{L_{\alpha_1+2}}$, ω_3 , $S_{\alpha_1+2,3}$, f_{23} and f_{13} , with uncertainties required to get the uncertainty in σ_{L_3} are given in Table 7. Values of f_{12} , σ_{L_1} and σ_{L_2} along with uncertainties are taken from Table 5 and Table 6, respectively. The values of σ_{L_3} along with the uncertainties are given in Table 7.

Lastly, total L-shell ionization (σ_L) and its uncertainty are given as under:

$$\sigma_L = \sum_i \sigma_{L_i} = \sigma_{L_1} + \sigma_{L_2} + \sigma_{L_3} \quad (19)$$

$$\left(\frac{\delta\sigma_L}{\sigma_L}\right)^2 = \left(\frac{\sigma_{L_1}}{\sigma_L}\right)^2 \left(\frac{\delta\sigma_{L_1}}{\sigma_{L_1}}\right)^2 + \left(\frac{\sigma_{L_2}}{\sigma_L}\right)^2 \left(\frac{\delta\sigma_{L_2}}{\sigma_{L_2}}\right)^2 + \left(\frac{\sigma_{L_3}}{\sigma_L}\right)^2 \left(\frac{\delta\sigma_{L_3}}{\sigma_{L_3}}\right)^2 \quad (20)$$

We have given σ_L as a function of energies in Table 8. Now, we know the measured $\sigma_{L_{1,2,3,L}}$ along with their correct uncertainties involved so that we can make use of these with right confidence.

Table 7: σ_{L_3} (barns/atom) along with uncertainties for various target atoms by Si beams of 84 MeV. Corresponding values of $\sigma_{L_{\alpha_1+\alpha_2}}$ (barns/atom) [40], conversion parameters (ω_3 , f_{23} , f_{13} [79, 80]) and $S_{\gamma_{1+5,2}}$ [59] are also given (uncertainties are given in percentage).

El.	$\sigma_{L_{\alpha_1+\alpha_2}}$	ω_3	$S_{\alpha_1+\alpha_2,3}$	f_{23}	f_{13}	σ_{L_3}
${}_{73}\text{Ta}$	6614 ± 11	0.251 ± 5	0.8000 ± 1	0.134 ± 10	0.328 ± 15	29844 ± 13
${}_{78}\text{Pt}$	5542 ± 11	0.303 ± 5	0.7831 ± 1	0.126 ± 10	0.545 ± 20	19175 ± 16
${}_{90}\text{Th}$	1537 ± 11	0.424 ± 5	0.7485 ± 1	0.103 ± 10	0.62 ± 15	3962 ± 17
${}_{92}\text{U}$	1099 ± 11	0.444 ± 5	0.7437 ± 1	0.14 ± 5	0.62 ± 15	2756 ± 16

Table 8: Values of total L shell ionization cross-section σ_L (barns/atom) along with uncertainties of various target atoms by Si beams of different energies (uncertainties are given in percentage).

El.	84 MeV	90 MeV	98 MeV	107 MeV	118 MeV	128 MeV	140 MeV
${}_{73}\text{Ta}$	42213 \pm 10	53086 \pm 10	64543 \pm 10	76243 \pm 10	167575 \pm 10	191674 \pm 10	198142 \pm 10
${}_{78}\text{Pt}$	29378 \pm 13	30303 \pm 13	38547 \pm 13	49786 \pm 13	95815 \pm 13	99213 \pm 14	107667 \pm 15
${}_{90}\text{Th}$	5905 \pm 14	7186 \pm 14	9024 \pm 14	13166 \pm 14	21059 \pm 14	25499 \pm 14	30782 \pm 14
${}_{92}\text{U}$	3992 \pm 14	4394 \pm 14	6173 \pm 14	7956 \pm 14	13377 \pm 14	15819 \pm 14	20089 \pm 14

4. Discussions on the salient results

The uncertainty in σ_{L_1} as given in Table 5 for ${}_{73}\text{Ta}$ is about 19%, where that of ${}_{78}\text{Pt}$ it is 32%, and those of ${}_{90}\text{Th}$ and ${}_{92}\text{U}$ it is about 37%; even though the uncertainty in $\sigma_{L_{\gamma_{2+3}}}$ is about 12%. **It is thus clear from the results that the uncertainty in σ_{L_1} is primarily dictated by the large uncertainty in ω_1 as given in Table 5.** In the case of σ_{L_2} the uncertainties are between 15 – 17% for elements ${}_{73}\text{Ta}$, ${}_{78}\text{Pt}$, ${}_{90}\text{Th}$ and ${}_{92}\text{U}$ (Table 6). It means the uncertainties are quite close to the uncertainty found in $\sigma_{L_{\gamma_{1+5}}}$ 12%. It happens because of small uncertainty (5%) in ω_2 . One important point is to note here that large uncertainty in f_{12} does not affect the overall uncertainty in σ_{L_2} because of weighted uncertainty propagation rule. We can notice that the value of f_{12} is rather more important than the associated uncertainty because of the weighted factor changes with its contribution.

The above trend seen with σ_{L_2} plays a similar role in propagating the uncertainty in σ_{L_3} . Here also, the uncertainties are between 13 – 17% for all four elements ${}_{73}\text{Ta}$, ${}_{78}\text{Pt}$, ${}_{90}\text{Th}$ and ${}_{92}\text{U}$. Since the first term containing fluorescence yield ω_3 and the fraction of radiative transition rates $S_{\alpha_{1+2,3}}$ along with production cross-section $\sigma_{L_{\alpha_{1+2}}}$ in Eqs. (10) gives major contribution, the uncertainty associated with this part is the main source of uncertainty. Further, uncertainty in ω_3 is not much (5%) and that in $S_{\alpha_{1+2,3}}$ is only 1%, hence, the uncertainty in σ_{L_3} is closed to that in $\sigma_{L_{\alpha_{1+2}}}$. Though the uncertainty in f_{23} and f_{13} are about 10 and 15%, respectively, still their share in uncertainty propagation is small because their contributions in Eqs. (10) (part 2 and 3), are small. Let us now list the uncertainty message on the L subshell ionization cross-sections reported earlier in Table 9.

Uncertainty in all L subshell ionization cross-sections cannot be equal, because the uncertainty in σ_{L_1} is always larger due to larger uncertainty in ω_1 than that in ω_2 and ω_3 . The uncertainty for σ_{L_2} and σ_{L_3} are nearly equal and highest uncertainty is with σ_{L_1} . These facts are well represented by the present work shown in Table 9. However, many cases shown in Table 9 do not support these facts. Hence, only some measurements treat the uncertainty associated with the L subshell ionization quite reasonably. This scenario is a deterrent for improving the theoretical understanding of the concerned complex mechanism. To give a correct treatment one has to follow elaborate error analysis as demonstrated in the present work. Having done this, one can confidently test the theories and look for any new physical processes if occurred in the experiment.

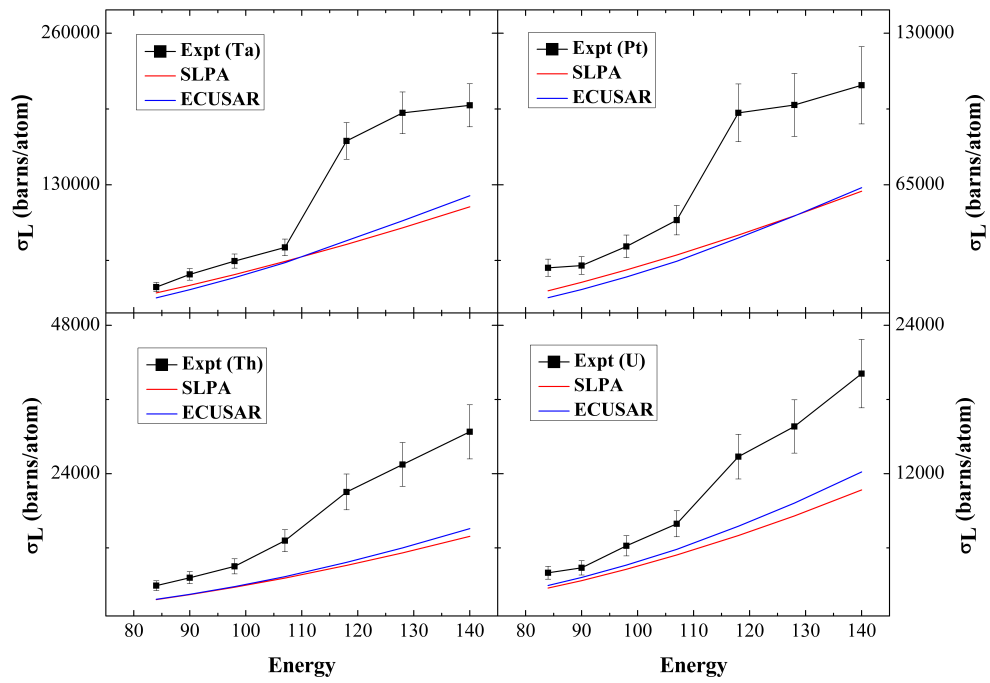


Figure 2: Total ionization cross-section vs bombarding energy of Si ion on various target Ta, Pt, Th and U. Measured data have been compared with ECUSAR [45] and SLPA theory [81].

Table 9: Comparison of uncertainties (%) quoted for L shell ionization cross sections in the previous experiments and present study.

Ref.	Targets	Uncertainty for	Projectile, its energy	Uncertainties (%)	Remarks
Palinkas and Schlenk [51]	Au, Pb, Bi	electron, 60-600 keV	$\sigma_{L_1}, \sigma_{L_2}, \sigma_{L_3}$	22, 15, 11	Fair treatment made
Carvalho <i>et al.</i> [53]	W	electron, 12-40 keV	$\sigma_3/\sigma_2, \sigma_2/\sigma_1$	10	σ_3/σ_2 must have lower error than that in σ_2/σ_1
Reusch <i>et al.</i> [52]	$29 \leq Z \leq 79$	electron, 50-200 keV	$\sigma_{L_1}, \sigma_{L_2}, \sigma_{L_3}, \sigma_L$	7-15, 6-15, 6-15, 15	Error in σ_{L_1} is underestimated
Bernstein and Lewis [62]	Ta, Au, Pb, U	H, 1.5-4.25 MeV	σ_{L_x}	20	No uncertainty message on L subshell ionization cross sections
Chang <i>et al.</i> [63]	Ta, Au, Bi	H, 1 to 5.5 and He, 1 to 11 MeV	$\sigma_{L_1}, \sigma_{L_2}, \sigma_{L_3}$	22, 28, 21	Uncertainty for L_2 cannot be higher than L_1
Semaniak <i>et al.</i> [68]	Between La to Au	$^{14}N, 1.75-22.4$ MeV	$\sigma_{L_1}, \sigma_{L_2}, \sigma_{L_3}$	10-25% for low energies and 10% for higher energies	All subshells cannot have same uncertainty
Somaniak <i>et al.</i> [69]	$72 \leq Z \leq 90$	C and N, 0.4 to 1.8 MeV/amu	$\sigma_{L_1}, \sigma_{L_2}, \sigma_{L_3}$	6-20, 5-12, 4-10	Achieving uncertainty as low as 4% for σ_{L_3} is doubtful
Dhal <i>et al.</i> [70]	Au, Bi	B, 4.8-8.8 MeV	$\sigma_{L_1}, \sigma_{L_2}, \sigma_{L_3}$	10% for both elements.	All subshells cannot have same uncertainty
Banas <i>et al.</i> [71]	Au	O of 0.4-2.2 MeV/amu	$\sigma_{L_1}, \sigma_{L_2}, \sigma_{L_3}$	15-30% for all subshell	Large error for σ_{L_1} and small for σ_{L_2} and σ_{L_3} is correct
Fijał-Kirjczyk <i>et al.</i> [73]	Au and Bi	S, 12.8-120 MeV	$\sigma_{L_1}, \sigma_{L_2}, \sigma_{L_3}$	10-30% for all subshell	Large error for σ_{L_1} and small for σ_{L_2} and σ_{L_3} is correct
Oswal <i>et al.</i> [40]	Ta, Pt, Th, U	Si, 84-140 MeV	$\sigma_{L_1}, \sigma_{L_2}, \sigma_{L_3}$	15-20% for Ta and 30-35% for others, 12-15, 12-15	Good estimation
Present work	Ta, Pt, Th, U	Si, 84-140 MeV	σ_L	10% for Ta, 13-15% for Pt and 14% for Th and U	correct treatment made
Present work	Ta	Si, 84 MeV	$\sigma_{L_1}, \sigma_{L_2}, \sigma_{L_3}$	19%, 16% and 13%	Shown for a specific energy
Present work	Pt	Si, 84 MeV	$\sigma_{L_1}, \sigma_{L_2}, \sigma_{L_3}$	32%, 17% and 16%	Shown for a specific energy
Present work	Th	Si, 84 MeV	$\sigma_{L_1}, \sigma_{L_2}, \sigma_{L_3}$	37%, 15% and 17%	Shown for a specific energy
Present work	U	Si, 84 MeV	$\sigma_{L_1}, \sigma_{L_2}, \sigma_{L_3}$	37%, 15% and 16%	Shown for a specific energy

The above methodology of error propagation can in principle be followed for future experiments. It can also be applied to earlier experiments if either data are still available for reanalysis or the production cross-section and its uncertainty are given in the concerned publications. However, the best available set of atomic parameters will be used to obtain L subshell ionization cross-sections from the L shell x-ray production cross-sections. Barros *et al.* [55] have discussed this issue recently in great detail. The atomic parameters are the main source of uncertainty, especially the fluorescence yields. Till date, ω_2 and ω_3 are mostly known within 5%, but ω_1 is having large uncertainty in particular towards the heavier target side. This is the reason for the larger uncertainty in σ_{L_1} in heavy atoms Th, U, etc. Though Coster-Kronig rates contain large uncertainty, but they do not affect much the L subshell cross-section because of their minor contribution (Eqs. (10)). Thanks to the theoretical advancements that the emission rates for the electric dipole transitions are known with almost no uncertainty (0.2%).

Plots of the total L shell ionization cross-section σ_L along with uncertainty versus the projectile energy (Fig. 2) as given in Table 8 exhibit an unusual feature. The σ_L behaves similarly, as the theoretical trend predicted by ECUSAR [45] and SLPA [81] up to a certain energy ≈ 100 MeV and takes a rise beyond this till it reaches a saturated value. Since we have dealt with the associated uncertainty in the measurement correctly, we can rely on the trend and infer on the concerned mechanism confidently. However, it is a nontrivial and requires a detail study that we keep for an interesting future investigation.

5. Suggestion on making accurate L subshell cross section measurements

Of course on the experimental side, statistical uncertainty is an important issue for any measurements, in our case, it is L shell x-ray production cross-sections from which L subshell ionization cross-sections are derived. In this case, some other issues are more vital than the statistical uncertainty. For example, detector efficiency is the major source of uncertainty. Hence, final uncertainty on the L shell x-ray production cross-sections depend on the individual uncertainty on various measurements such as detector efficiency, counting statistics, number of incident ions and target thickness and target contamination. Let us discuss how the uncertainty of these experimental

parameters can be kept minimum. We will make an attempt to find the best possible way of making the most accurate L shell x-ray production cross-section measurements below.

First, we consider measurement of the detector efficiency of x-ray semiconductor detector used for x-ray production cross-sections. There are several efficiency measurements, for example, Barfoot *et al.* [82], Tribedi and Tandon [83], Mohanty *et al.* [75], Kumar *et al.* [84]. It is shown there that efficiency for a high purity germanium (HPGe) detector can be known within 5% [85], for a Si(Li) detector within 6% [75], and expected to get similar accuracy for a silicon drift detector (SDD) [86]. Hence, at this point, one can measure the detector efficiency within 5-6%. Absolute efficiency of the detector depends not only on detector properties discussed but also on the correct position and solid angle called geometrical efficiency. To define it well, a collimator with a dimension smaller than the detector crystal size in front of the detector is normally used [84].

Next, we discuss the measurement of the number of projectile-ions bombarded on the target. Since charge state of the heavy projectile-ions is changed to a good extent during the ion-solid collisions, charge collected in Faraday cage cannot give correct counting of incident particles. One must follow any one of the following techniques to have less than 1% uncertainty: (i) elastically scattered projectiles from a heavy target like gold [87], keeping the whole scattering chamber electrically isolated for using it as a Faraday cup [88], using two Faraday cups one in front of the target and another behind the target [89]. Target thickness, as well as target contamination, can be correctly measured with Rutherford back-scattering technique [90].

6. Crystal spectrometer vs semiconductor x-ray detector in measuring L subshell cross section

High-resolution studies using crystal spectrometers help us know precisely the characteristic line energies. However, such efforts do not improve the accuracy of the L subshell ionization because in high-resolution cases, we need only the emission rates, the fraction of radiative transition rates has no role over here. Since emission rates are very accurate (within 0.2 %) and thus the fraction of radiative transition rates, as discussed above, does not introduce considerable uncertainty at all. Hence, experiments performed with crystal spectrometers, for example [52, 53, 54], reported exactly similar

uncertainty message as the studies using semiconductor x-ray detectors do.

7. Conclusion

We always gain a good understanding of any physical process by comparing the experimental data with the theoretical values. The comparison is meaningful only if the uncertainty in experiment and theory is accounted to the best possible level. However, it is seldom seen that the theoretical works talk any thing about the uncertainty in the calculation. Often, we can find experimental studies quote these uncertainties, however, most of the time the uncertainties are not estimated correctly, especially for a complex phenomenon. We have taken a test case through L subshell ionization of atoms by particle or photon impact. Experimentally, measured x-ray production cross-sections are used to obtain the ionization cross-sections, which are theoretically calculated. Furthermore the uncertainty of the x-ray production cross-section is mainly governed by statistics (Type A uncertainty) and detector efficiency (Type B uncertainty) but the ionization cross-section involves many atomic parameters (systematic uncertainty) having a wide uncertainty spectrum. Consequently, determining the measurement uncertainty in the L subshell ionization cross-section is always quite complex. We have thoroughly studied this issue in a systematic manner, where the rule of the weighted propagation of the uncertainty is introduced so that on every occasion, percentage uncertainty can be used. We notice that σ_{L_1} suffers from the maximum uncertainty because of a large uncertainty in the best fluorescence parameters (systematic uncertainty) available till date relevant to L_1 ($2s_{1/2}$) subshell compared to those associated with the other two subshells L_2 ($2p_{1/2}$) and L_3 ($2p_{3/2}$). Hence, a comparison between the theory and experiment would give higher importance to L_2 and L_3 subshell ionisation cross-sections because of smaller measurement uncertainty than that in L_1 .

Sometimes the measured data show a certain departure from the usual trend indicating certain unexplored mechanism. Nevertheless, a lack of confidence in associated uncertainties forbids one to unfold the mystery. At such juncture, log scale is used so that the data may look smoother than when it is on a linear scale, and thus any excessive scatter or unusual trend can be less noticeable. In contrast, accurate uncertainty analysis gives us full confidence about the data, and thus one will not hesitate to draw any meaningful inference if any departure is seen with the measured data. Furthermore, proper

uncertainty analysis teaches us the best possible care that can be taken for the improved measurements. Thus, we have suggested a novel way by which the reliable and accurate L subshell ionization cross-section data can be obtained. Finally, we believe this work provides a general overview to every researcher that the uncertainty aspect must be taken into utmost care for right advancement of science.

8. Credit authorship contribution statement

Shashank Singh: Methodology, calculation, preparation of Tables and figures, Soumya Chatterjee: Methodology, calculation, preparation of Tables and figures, D. Mitra: Formal analysis, methodology, validation, and T. Nandi: Conceptualization, methodology, supervision, validation, visualization, writing - original draft, writing - review and editing.

9. Acknowledgments

One of the authors (S.S.) gratefully acknowledges his supervisors K.P. Singh, Mumtaz Oswal and B. R. Behera for their support to work with any other experts freely for widening his exposures. We gratefully acknowledge Adedamola David Aladese for checking the manuscript thoroughly and giving invaluable comments.

References

- [1] R. Dybkaer, Accreditation and quality assurance **16**, 479 (2011).
- [2] J. Choi, E. Hwang, H.-Y. So, and B. Kim, Accreditation and quality assurance **8**, 13 (2003).
- [3] S. A. Bell, (2001).
- [4] I. BIPM, I. IFCC, I. ISO, and O. IUPAP, Joint Committee for Guides in Metrology (2008).
- [5] E. Burhop and H. Massey, in *Mathematical Proceedings of the Cambridge Philosophical Society*, Vol. 36 (Cambridge University Press, 1940) pp. 43–52.

- [6] D. Rester and W. Dance, *Physical Review* **152**, 1 (1966).
- [7] K. J. Nygaard, *Phys. Rev. A* **11**, 1475 (1975).
- [8] Y. Hahn, *Phys. Rev. Lett.* **39**, 82 (1977).
- [9] D. Bote and F. Salvat, *Phys. Rev. A* **77**, 042701 (2008).
- [10] Y. Liu, Z. Xu, X. Wang, and L. Zeng, *Nuclear Instruments and Methods in Physics Research Section B: Beam Interactions with Materials and Atoms* **446**, 1 (2019).
- [11] J. Zhao, S. Bai, Z. An, J. Zhu, W. Tan, and M. Liu, *Radiation Physics and Chemistry* **171**, 108722 (2020).
- [12] L. Tian, C. Dai, B. Fang, and Y. Liu, *Nuclear Instruments and Methods in Physics Research Section B: Beam Interactions with Materials and Atoms* **471**, 84 (2020).
- [13] E. Storm and H. I. Israel, *Photon cross sections from 0.001 to 100 MeV for elements 1 through 100.*, Tech. Rep. (Los Alamos Scientific Lab., N. Mex., 1967).
- [14] W. Veigele, *Atomic Data and Nuclear Data Tables* **5**, 51 (1973).
- [15] K. Shatendra, K. L. Allawadhi, and B. S. Sood, *Phys. Rev. A* **31**, 2918 (1985).
- [16] S. Singh, D. Mehta, S. Kumar, M. L. Garg, N. Singh, P. C. Mangal, and P. N. Trehan, *X-Ray Spectrometry* **18**, 193 (1989), <https://onlinelibrary.wiley.com/doi/pdf/10.1002/xrs.1300180503> .
- [17] K. S. Mann, N. Singh, R. Mittal, B. S. Sood, and K. L. Allawadhi, *X-Ray Spectrometry* **23**, 208 (1994), <https://onlinelibrary.wiley.com/doi/pdf/10.1002/xrs.1300230505> .
- [18] M. Ertuğrul, *Zeitschrift für Physik D Atoms, Molecules and Clusters* **38**, 91 (1996).
- [19] J. D. GARCIA, E. GERJUOY, and J. E. WELKER, *Phys. Rev.* **165**, 66 (1968).

- [20] J. Garcia, *Physical Review A* **1**, 280 (1970).
- [21] R. D. DuBois, L. H. Toburen, and M. E. Rudd, *Phys. Rev. A* **29**, 70 (1984).
- [22] R. D. DuBois and S. T. Manson, *Phys. Rev. A* **35**, 2007 (1987).
- [23] M. H. Chen and B. Crasemann, *Atomic Data and Nuclear Data Tables* **41**, 257 (1989).
- [24] M. Pajek, A. P. Kobzev, R. Sandrik, A. V. Skrypnik, R. A. Ilkhamov, S. H. Khusmurodov, and G. Lapicki, *Phys. Rev. A* **42**, 261 (1990).
- [25] C. Montanari and J. Miraglia, *Nuclear Instruments and Methods in Physics Research Section B: Beam Interactions with Materials and Atoms* **407**, 236 (2017).
- [26] J. Miranda, D. Serrano, J. Pineda, D. Marín-Lámbarri, L. Acosta, J. Mendoza-Flores, S. Reynoso-Cruces, and E. Chávez, *Nuclear Instruments and Methods in Physics Research Section B: Beam Interactions with Materials and Atoms* (2019), <https://doi.org/10.1016/j.nimb.2019.06.046>.
- [27] P. D. Pérez, T. P. R. Cabello, J. C. Trincavelli, and S. Suárez, *Radiation Physics and Chemistry* **154**, 21 (2019).
- [28] J. M. Hansteen and O. P. Mosebekk, *Phys. Rev. Lett.* **29**, 1361 (1972).
- [29] J. Andersen, E. Lægsgaard, M. Lund, and C. Moak, *Nuclear Instruments and Methods* **132**, 507 (1976).
- [30] R. Anholt, W. E. Meyerhof, C. Stoller, E. Morenzoni, S. A. Andriamonje, J. D. Molitoris, O. K. Baker, D. H. H. Hoffmann, H. Bowman, J. S. Xu, Z. Z. Xu, K. Frankel, D. Murphy, K. Crowe, and J. O. Rasmussen, *Phys. Rev. A* **30**, 2234 (1984).
- [31] M. Sarkar, D. Bhattacharya, M. Chatterjee, P. Sen, G. Kuri, D. Mahapatra, and G. Lapicki, *Nuclear Instruments and Methods in Physics Research Section B: Beam Interactions with Materials and Atoms* **103**, 23 (1995).

- [32] Y. Singh, D. Mitra, L. C. Tribedi, and P. Tandon, *Physical Review A* **63**, 012713 (2000).
- [33] Y. P. Singh, D. Misra, U. Kadhane, and L. C. Tribedi, *Phys. Rev. A* **73**, 032712 (2006).
- [34] M. Msimanga, C. Pineda-Vargas, and M. Madhuku, *Nuclear Instruments and Methods in Physics Research Section B: Beam Interactions with Materials and Atoms* **380**, 90 (2016).
- [35] H. Verma, *Radiation Physics and Chemistry* **150**, 30 (2018).
- [36] I. Gorlachev, V. Alexandrenko, N. Gluchshenko, I. Ivanov, A. Kireyev, M. Krasnopyorova, A. Kurakhmedov, A. Platov, and M. Zdorovets, *Nuclear Instruments and Methods in Physics Research Section B: Beam Interactions with Materials and Atoms* **430**, 31 (2018).
- [37] L. Chang-Hui, Z. Xiao-An, L. Yao-Zong, Z. Yong-Tao, Z. Xian-Ming, W. Xing, M. Ce-Xiang, and X. Guo-Qing, *Acta Physica Sinica* **67** (2018).
- [38] M. Oswal, S. Kumar, U. Singh, G. Singh, K. Singh, D. Mehta, D. Mitnik, C. C. Montanari, and T. Nandi, *Nuclear Instruments and Methods in Physics Research Section B: Beam Interactions with Materials and Atoms* **416**, 110 (2018).
- [39] H. Silhadi, S. Fazinic, A. Haidra, I. Zamboni, and S. Ouziane, *Nuclear Instruments and Methods in Physics Research Section B: Beam Interactions with Materials and Atoms* **459**, 158 (2019).
- [40] M. Oswal, S. Kumar, U. Singh, G. Singh, K. Singh, D. Mehta, A. Méndez, D. Mitnik, C. Montanari, D. Mitra, and T. Nandi, *Radiation Physics and Chemistry* , 108809 (2020).
- [41] L. Kocbach, J. Hansteen, and R. Gundersen, *Nuclear Instruments and Methods* **169**, 281 (1980).
- [42] E. Merzbacher and H. W. Lewis, (1958).
- [43] W. Brandt and G. Lapicki, *Physical Review A* **20**, 465 (1979).
- [44] W. Brandt and G. Lapicki, *physical review A* **23**, 1717 (1981).

- [45] G. Lapicki, Nuclear Instruments and Methods in Physics Research Section B: Beam Interactions with Materials and Atoms **189**, 8 (2002).
- [46] W. Brandt and G. Lapicki, Phys. Rev. A **20**, 465 (1979).
- [47] W. Brandt and G. Lapicki, Phys. Rev. A **23**, 1717 (1981).
- [48] J. E. Miraglia and M. S. Gravielle, Phys. Rev. A **67**, 062901 (2003).
- [49] C. Merlet, X. Llovet, and F. Salvat, Physical Review A **69**, 032708 (2004).
- [50] C.-N. Chang, Phys. Rev. A **19**, 1930 (1979).
- [51] J. Palinkas and B. Schlenk, Zeitschrift für Physik A Atoms and Nuclei **297**, 29 (1980).
- [52] S. Reusch, H. Genz, W. Löw, and A. Richter, Zeitschrift für Physik D Atoms, Molecules and Clusters **3**, 379 (1986).
- [53] M. L. Carvalho, J. G. Ferreira, and L. Salgueiro, Phys. Rev. A **37**, 106 (1988).
- [54] X. Llovet, C. J. Powell, F. Salvat, and A. Jablonski, Journal of Physical and Chemical Reference Data **43**, 013102 (2014).
- [55] S. Barros, V. Vanin, N. Maidana, and J. Fernández-Varea, Journal of Physics B: Atomic, Molecular and Optical Physics **48**, 175201 (2015).
- [56] P. V. Rao, M. H. Chen, and B. Crasemann, Physical Review A **5**, 997 (1972).
- [57] M. Kolbe, P. Hönicke, M. Müller, and B. Beckhoff, Physical Review A **86**, 042512 (2012).
- [58] J. H. Scofield, Physical Review A **9**, 1041 (1974).
- [59] J. Campbell and J.-X. Wang, Atomic data and nuclear data tables **43**, 281 (1989).
- [60] M. O. Krause, Journal of physical and chemical reference data **8**, 307 (1979).

- [61] J. H. Scofield, *Atom. Data Nucl. Data Tabl.* **14**, 121 (1974).
- [62] E. M. Bernstein and H. Lewis, *Physical Review* **95**, 83 (1954).
- [63] C. N. Chang, J. F. Morgan, and S. L. Blatt, *Phys. Rev. A* **11**, 607 (1975).
- [64] C. V. B. Leite, N. V. d. C. Faria, and A. G. de Pinho, *Phys. Rev. A* **15**, 943 (1977).
- [65] R. Wheeler, R. Chaturvedi, and S. Amey, *IEEE Transactions on Nuclear Science* **26**, 1166 (1979).
- [66] R. Sokhi and D. Crumpton, *Atomic data and nuclear data tables* **30**, 49 (1984).
- [67] J. Miranda and G. Lapicki, *Atomic data and nuclear data tables* **100**, 651 (2014).
- [68] J. Semaniak, J. Braziewicz, T. Czyzewski, L. Głowacki, M. Haller, M. Jaskóła, R. Karschnick, A. Kobzev, M. Pajek, W. Kretschmer, *et al.*, *Nuclear Instruments and Methods in Physics Research Section B: Beam Interactions with Materials and Atoms* **86**, 185 (1994).
- [69] J. Semaniak, J. Braziewicz, M. Pajek, T. Czyżewski, L. Głowacka, M. Jaskóła, M. Haller, R. Karschnick, W. Kretschmer, Z. Halabuka, and D. Trautmann, *Phys. Rev. A* **52**, 1125 (1995).
- [70] B. Dhal, T. Nandi, and H. Padhi, *Nuclear Instruments and Methods in Physics Research Section B: Beam Interactions with Materials and Atoms* **101**, 327 (1995).
- [71] D. Banas, J. Braziewicz, M. Pajek, J. Semaniak, T. Czyżewski, I. Fijał, M. Jaskóła, W. Kretschmer, T. Mukoyama, and D. Trautmann, *Journal of Physics B: Atomic, Molecular and Optical Physics* **35**, 3421 (2002).
- [72] M. Pajek, D. Banaś, J. Semaniak, J. Braziewicz, U. Majewska, S. Chojnacki, T. Czyżewski, I. Fijał, M. Jaskóła, A. Glombik, *et al.*, *Physical Review A* **68**, 022705 (2003).

- [73] I. Fijał-Kirejczyk, M. Jaskóła, A. Korman, D. Banaś, J. Braziewicz, J. Choiński, U. Majewska, M. Pajek, W. Kretchmer, G. Lapicki, *et al.*, Nuclear Instruments and Methods in Physics Research Section B: Beam Interactions with Materials and Atoms **266**, 2255 (2008).
- [74] D. Creagh and J. Hubbell, Acta Crystallographica Section A: Foundations of Crystallography **46**, 402 (1990).
- [75] B. Mohanty, P. Balouria, M. Garg, T. Nandi, V. Mittal, and I. Govil, Nuclear Instruments and Methods in Physics Research Section A: Accelerators, Spectrometers, Detectors and Associated Equipment **584**, 186 (2008).
- [76] M. Berger, J. Hubbell, S. Seltzer, J. Chang, J. Coursey, R. Sukumar, D. Zucker, and K. Olsen, URL <http://physics.nist.gov/PhysRefData/Xcom/Text/XCOM.html> (2010).
- [77] E. Tıraşoğlu and Ö. Söğüt, Pramana **70**, 471 (2008).
- [78] H. Rahangdale, D. Mitra, P. Das, S. De, M. Guerra, J. Santos, and S. Saha, Journal of Quantitative Spectroscopy and Radiative Transfer **174**, 79 (2016).
- [79] J. Campbell, Atomic Data and Nuclear Data Tables **85**, 291 (2003).
- [80] J. Campbell, Atomic Data and Nuclear Data Tables **95**, 115 (2009).
- [81] C. Montanari, D. Mitnik, and J. Miraglia, Radiation Effects & Defects in Solids **166**, 338 (2011).
- [82] K. Barfoot, I. Mitchell, L. Avaldi, H. Eschbach, and W. Gilboy, Nuclear Instruments and Methods in Physics Research Section B: Beam Interactions with Materials and Atoms **5**, 534 (1984).
- [83] L. Tribedi and P. Tandon, Nuclear Instruments and Methods in Physics Research Section B: Beam Interactions with Materials and Atoms **69**, 178 (1992).
- [84] S. Kumar, U. Singh, M. Oswal, G. Singh, N. Singh, D. Mehta, T. Nandi, and G. Lapicki, Nuclear Instruments and Methods in Physics Research Section B: Beam Interactions with Materials and Atoms **395**, 39 (2017).

- [85] C. M. Salgado, C. C. Conti, and P. H. Becker, Applied radiation and isotopes **64**, 700 (2006).
- [86] X. Zhou, R. Cheng, Y. Zhao, Y. Wang, Y. Lei, Y. Chen, X. Ma, and G. Xiao, Scientific reports **9**, 1 (2019).
- [87] T. Nandi, P. Marketos, P. Joshi, R. Singh, C. Safvan, P. Verma, A. Mandal, A. Roy, and R. Bhowmik, Physical Review A **66**, 052510 (2002).
- [88] S. Narvekar, R. Hosangadi, L. Tribedi, R. Pillay, K. Prasad, and P. Tandon, Pramana **39**, 79 (1992).
- [89] X. Zhou, Y. Zhao, R. Cheng, Y. Wang, Y. Lei, X. Wang, and Y. Sun, Nuclear Instruments and Methods in Physics Research Section B: Beam Interactions with Materials and Atoms **299**, 61 (2013).
- [90] L. C. Feldman and J. W. Mayer, North Holland, Elsevier Science Publishers, P. O. Box 211, 1000 AE Amsterdam, The Netherlands, 1986. (1986).